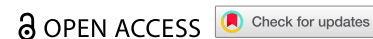



ORIGINAL RESEARCH



Humanized mouse models of *KRAS*-mutated colorectal and pancreatic cancers with HLA-class-I match for pre-clinical evaluation of cancer immunotherapies

Maria E. Davola, Olga Cormier, Madeleine Lepard, Jamie McNicol, Susan Collins, Joanne A. Hammill, Christopher Silvestri, Jonathan L. Bramson, Amy Gillgrass, and Karen L. Mossman 

Department of Medicine, Centre for Discovery in Cancer Research and McMaster Immunology Research Centre, McMaster University, Hamilton, ON, Canada

ABSTRACT

Cancer immunotherapy promises to treat challenging cancers including *KRAS*-mutated colorectal cancer (CRC) and pancreatic ductal adenocarcinoma (PDAC). However, pre-clinical animal models that better mimic patient tumor and immune system interactions are required. While humanized mice are promising vehicles for pre-clinical immunotherapy testing, currently used cancer models retain limitations, such as lack of a human thymus for human leukocyte antigen (HLA)-based education of human T cells. As cytotoxic T lymphocyte (CTL) activity underlies many immunotherapies, we developed more clinically relevant *KRAS*-mutated CRC and PDAC humanized cancer models using transgenic NRG-A2 mice expressing HLA-A2.1 to enable HLA-class-I match between mouse tissues (including the thymus), the humanized immune system and human tumors. Using these novel humanized cancer models and a CTL-mediated combination (immuno)therapy with clinical potential, we were able to recapitulate the complexity and therapy-induced changes reported in patient biopsies, demonstrating the use of these HLA-matched models for pre-clinical validation of novel immunotherapies.

ARTICLE HISTORY

Received 7 June 2024
Revised 17 December 2024
Accepted 24 February 2025

KEYWORDS

Cancer immunotherapy; colorectal cancer; HLA class I match; HLA-A2.1; humanized cancer model; humanized mice; immune checkpoint inhibitors; *KRAS*; NRG-A2; pancreatic ductal adenocarcinoma



Introduction


Immunotherapy has taken the main stage in cancer treatment given striking increases in survival and quality of life for patients. Worldwide, *KRAS* mutations represent ~45% and 90% of colorectal cancer (CRC) and pancreatic ductal adenocarcinoma (PDAC) cases, respectively, cancers poorly responsive to conventional therapies or *KRAS*-targeting. Although immune checkpoint inhibitor (ICI) efficacy in CRC and PDAC is limited, combination (immuno)therapies show promise in clinical studies.^{1,2} Immunotherapies use the patient's immune system to induce anti-tumor responses. Modeling the tumor microenvironment (TME) is particularly important in understanding human tumor immunology and exploring novel immunotherapies. Existing pre-clinical mouse models have poor predictive value as they fail to recapitulate human immunology, tumor biology and TME dynamics. Given clinical trial costs and complexities, "development of pre-clinical models that translate to human immunity" was identified as the #1 key challenge for cancer immunotherapy.³

Humanized mice (hu-mice), immunocompromised mice engrafted with human immune components, are being developed to recapitulate the human immune system in a mouse.⁴ Injection of human peripheral blood mononuclear cells (PBMCs) or lymphocytes (PBLs) is relatively straightforward, although while T cells survive engraftment, B cells are maintained at very low levels, and innate cell populations including myeloid and NK cells only survive for the first few days.

Furthermore, high levels of mature human T cells in PBMC-derived hu-mice provoke acute graft-vs-host disease (GvHD), limiting experiment length.⁴ To avoid GvHD, knockout mice deficient for MHC class I and II have been used.⁵ Mice engrafted with human CD34⁺ hematopoietic stem cells (HSCs) from cord or adult-mobilized blood develop a more complete hematopoietic system with innate and adaptive immune cells, low numbers of red blood cells and platelets, and significantly delayed GvHD development.⁴ However, a remaining limitation is the lack of a human thymus for human leukocyte antigen (HLA)-based education and selection of human T cells.⁴ One solution involves implanting autologous fragments of human fetal thymus and liver under the mouse kidney capsule and injecting fetal liver-derived CD34⁺ HSCs (BLT-hu-mouse model), the most complete yet complex hu-mouse model.

Another approach for HLA-mediated education of human T cells is the use of transgenic mice expressing HLA class I and/or II molecules.⁶ HLA-transgenic mice reconstituted with HLA-matched HSCs have increased breadth, frequency and engraftment of key cell populations including CD8⁺ and CD4⁺ T cells, resulting in enhanced antigen-specific immunity.⁶ As transgenic NRG-A2 mice expressing class I HLA-A2.1 develop more functional CD8⁺ T cells when reconstituted with HLA-A2.1-matched HSCs,⁷ this model would be more clinically relevant to study cancer immunotherapies where cytotoxic T lymphocytes (CTLs) are key

CONTACT Karen L. Mossman  mossk@mcmaster.ca  Department of Medicine, Centre for Discovery in Cancer Research and McMaster Immunology Research Centre, McMaster University, 1280 Main Street West, Hamilton, ON, L8S 4K1, Canada

 Supplemental data for this article can be accessed online at <https://doi.org/10.1080/2162402X.2025.2473163>

© 2025 The Author(s). Published with license by Taylor & Francis Group, LLC.

This is an Open Access article distributed under the terms of the Creative Commons Attribution-NonCommercial License (<http://creativecommons.org/licenses/by-nc/4.0/>), which permits unrestricted non-commercial use, distribution, and reproduction in any medium, provided the original work is properly cited. The terms on which this article has been published allow the posting of the Accepted Manuscript in a repository by the author(s) or with their consent.

players. To our knowledge, no cancer-related studies using HSC-derived humanized transgenic mice with HLA class I match have been published. Thus, our goal was to develop pre-clinical cancer models that better simulate the crosstalk between human CTLs and human tumors, to explore and validate novel immunotherapies. We established *KRAS*-mutated CRC and PDAC cancer models in NRG-A2 mice with complete tissue, tumor and immune system HLA-A2.1 match. Using a previously published CTL-mediated combination (immuno)therapy,⁸ we demonstrate the potential use of these humanized cancer models in immuno-oncology research.

Materials & methods

Animals

NOD-Rag1null IL2rgnull (NRG) mice were obtained from Jackson laboratories (Bar Harbor, ME, USA). NRG mice expressing human HLA-A2.1/A*02:01 (NRG-A2 or NOD.Cg-Rag1tm1Mom IL2rgtm1Wjl/SzJ X NOD.cg-Prkdcscid IL2rgtm1Wjl Tg (HLA-A2.1)1Enge/SzJ) were a generous gift from Dr Ali Ashkar (McMaster University, ON, Canada). Mice were housed in level 2 containment with ad libitum access to food and water, 12 h light cycle, 50%–60% humidity, and at 20–25°C room temperature. Experiments were approved by the McMaster Animal Research and Ethics Board in compliance with the Canadian Council on Animal Care (AUP# 211239).

Cell lines

Human colorectal HCT-116 cancer cells (NIH) were maintained in Roswell Park Memorial Institute (RPMI) medium supplemented with 1 mM L-glutamine and 10% fetal bovine serum (FBS). Human pancreatic CFPAC-1 cancer cells (ATCC) were maintained in Iscove's Modified Dulbecco's Medium (IMDM) supplemented with 10% FBS. Both cell lines were maintained at 37°C with 5% CO₂ and tested negative for Hepatitis A, B, C viruses, HIV-1, HIV-2, Mycoplasma and Corynebacterium bovis (Charles River). HCT-116 HLA-A2.1 knockout cells (HCT-HLAko) were generated by CRISPR gene editing using the Gene Knockout Kit (EditCo, formerly Synthego) following manufacturer's protocol. Guide sequences: ACAGCGACGCCGCGAGCCAG, CCUUC ACAUCCGUGUCUCC and UUCACAUCCGUGUCCC GGCC. MaxCyte gTX under the HCT116 protocol in the OC-25×3 Processing Assembly was used for electroporation of the complexed gRNA/Cas9 ribonucleoprotein. Knockout population was selected by FACS, and gene knockout was confirmed by flow cytometry.

Generation of humanized mice with HLA class I match

NRG-A2 mice were engrafted with CD34⁺ HSCs from human umbilical cord blood (HiREB approved ethics #13–813-T). CD34⁺ HSCs were isolated, screened for HLA-A2.1/A*02:01 alleles and engrafted as described.⁶ In brief, newborn (24–72 h old) NRG-A2 mice were irradiated twice with 3 cGy 3 hours

apart. 1×10^5 – 1×10^6 CD34⁺ HSCs were then injected intrahepatically in 30 µL phosphate-buffered saline (PBS).

Flow cytometry analysis

At different timepoints, 50 µL of blood was collected into EDTA-coated tubes. At endpoint, tumors were harvested, minced with a razor blade in RPMI 10% FBS media, digested with 50 µg/mL liberase (Sigma Aldrich 5401054001) for 1 h at 37°C with constant stirring and passed over a 100-micron filter. Erythrocytes from blood and tumor-derived cell suspensions were lysed using ACK lysis buffer (Quality Biological 118-156-101). Remaining cells were treated with anti-human Fc Receptor Binding Inhibitor and anti-mouse CD16/CD32 antibodies (Table S1). Cells were stained with an antibody cocktail followed by fixable viability dye (Table S1) and fixed with 4% paraformaldehyde or cytofix/cytoperm (BD Biosciences 554714). Samples were recorded on the Cytoflex LX flow cytometer (Beckman Coulter) equipped with a flow rate calibrator and analyzed using FlowJo software (version 10.7.1) (BD Biosciences). Mice with at least 5% or 25,000 per mL hCD45⁺ leukocytes in the blood at 16 weeks post-HSCs engraftment were selected for subsequent experiments (Tables S2–S5).

Tumor implantation and treatment

Male and female NRG or humanized NRG-A2 mice were subcutaneously implanted with 1×10^7 HCT-116 or CFPAC-1 cells resuspended in 200 µL of a 1:1 mixture PBS:Matrigel (Corning 356237) into the left flank. Tumors reached treatable size (50–100 mm³) 10 days post-implantation. Mice were randomized by tumor volume, reconstitution level, donor sample and gender into three groups: PBS, ICI and combination (immuno)therapy (Comb). Tumors were treated as described⁸ with slight modifications. For ICI, mice bearing tumors were treated intraperitoneally (i.p.) with human α-CTLA-4 (BioXcell BE0190) and α-PD-1 (BioXcell BE0188) antibodies from day 11 every 3 days until 10 doses total (200 µg of each antibody for dose 1; 100 µg of each for remaining doses in 200 µL PBS).^{9,10} For Comb, mice bearing tumors were treated intratumorally (i.t.) with 100 µg mitomycin c (MMC, Sigma-Aldrich M4287) in 50 µL sterile water at day 10; 2×10^7 pfu oncolytic bovine herpesvirus type 1 (oBoHV-1) i.t. at days 11, 14 and 17; and human ICI i.p. as above. Tumors were measured every 3–4 days using a digital caliper until reaching endpoint (525 mm³). Mice with a body weight loss higher than 20%, extended fur loss or abnormal appearance were humanely euthanized.

HLA-restricted tumor-specific cytotoxic activity of CD8⁺ T cells

To assess HLA-A2.1-restricted tumor recognition of CTLs, HLA-A2.1-matched hu-NRG-A2 mice bearing HCT-116 tumors were treated with Comb, and splenocytes were isolated day 20 post-implantation (day 10 post-treatment). Splenic CTLs were purified using positive CD8 Microbeads selection (Miltenyi Biotec 130-045-201) and co-cultured for

4 h with HCT-116 cells (ratio 1:2 CTLs-tumor cells) \pm α HLA-A2 antibody (ThermoFisher MA5-16586).⁷ CTLs were additionally co-cultured with HCT-HLAko. Expressions of HLA-A2.1 on tumor cells and CD69, Granzyme B (GrB) and Ki67 on CTLs were determined by flow cytometry as described above (Table S1).

Histology and multiplexed ion-beam imaging by time of flight (MIBI-TOF)

Tumors were resected, fixed in 10% formalin for 48 h and transferred to 70% ethanol until embedded in paraffin. 4- μ m sections were processed for hematoxylin and eosin (H&E) staining using Automated Leica Bond Rx stainer with Epitope Retrieval Buffer 2 (Leica, AR9640), and for MIBI-TOF staining as previously described.¹¹

MIBI-TOF image acquisition, processing, and analysis

Spectral images of 400 \times 400 μ m of stained tumor sections were collected as previously described.¹¹ Multiplexed raw image sets were denoised and aggregate filtered using IonPath's MIBI/O and the default correction settings. Processed image TIFF files represent the dataset. Cellular segmentation was performed with the input of nuclear-stained and membrane-stained marker channels using Mesmer and segmentation mask images were stored as TIFF files for further analysis in MATLAB and R Studio (Table S7).

Single-cell data were extracted for all cell objects defined by the segmentation masks using a custom R script and packages (Table S7). The mean intensity values per object were asinh-transformed with a cofactor of 1. To classify cell types based on marker expression levels, the Bioconductor 'FlowSOM' R package was used. The algorithm clustered 61,418 total cells from the cohort into 100 FlowSOM clusters. By inspecting a heatmap displaying normalized individual marker intensities, each of the 100 clusters was annotated into 7 cell types. CytoMAP software performed single-cell spatial analysis to determine the microenvironments present in the FOVs. The algorithm uses cell types and their positions in the image to find local compositions of cells within a circular area defined by a radius of 75 pixels from each cell in the image. The number of regions chosen for this dataset was empirically determined by investigating the effects of choosing from between 2 and 8 regions, revealing that a region number equal to four was most informative and representative of the 75 images and cell types present within them. The software calculated the number of cells in each neighborhood.

Statistical analysis

Student's t-test was used to compare two groups of data, while one-way ANOVA was performed to determine the difference among three or more groups. The null hypothesis was rejected for p-values less than 0.05. All data analyses were carried out using GraphPad Prism version 10.2.3.

Results

Establishment of a human KRAS-mutated CRC model in HLA-A2.1-matched humanized mice

Human colorectal HCT-116 cancer cells are well characterized with multiple mutations including KRAS^{G13D} and expression of class I HLA subtype A2.1.¹² Tumor growth of subcutaneously implanted HCT-116 cells was first evaluated in non-humanized NRG mice (non-hu-mice; Figure 1(a)). At endpoint, tumors were harvested and HLA-A2.1 expression on CK18⁺ tumor cells was determined by flow cytometry. Similar HLA-A2.1 levels were found in cultured cells and harvested tumors (Figure 1(b)) confirming that tumor development and growth do not affect HLA-A2.1 expression.

Transgenic NRG-A2 mice were reconstituted with HLA-A2.1-matched human cord blood-derived CD34⁺ HSCs (Figure 1(c)). Reconstitution levels were assessed at 12 weeks of age (Table S2) and reevaluated at 16 weeks (Table S2 and Figure 1(d)) to confirm sufficient immune reconstitution before tumor implantation in 18-week-old hu-mice (Figure 1(c)). Similar tumor growth (Figure 1(a)) and HLA-A2.1 expression (Figure 1(b)) were observed in non-hu-mice and hu-mice, as seen by others.^{13,14} To evaluate changes in reconstitution and immune cell abundance with tumor implantation, blood was collected at 16 weeks (12 days pre-implantation), 20 weeks (17 days post-implantation) and at endpoint (Figure 1(c)). Only one mouse showed a clear increase in reconstitution levels at day 17 (green triangle in Figure 1(d)), with overall reconstitution levels remaining stable in blood between day 17 and endpoint (Figure 1(d)). Moreover, CD8⁺ T cell levels in blood were significantly but transiently reduced after tumor implantation, fully recovering by endpoint (Figure 1(e) and Figure S1). At endpoint tumors were harvested to evaluate TME by flow cytometry. Tumors showed an increase of myeloid cells and a trend of a decrease in B cells relative to circulating blood (Figure 1(e) and Figure S1).

Combination (immuno)therapy in humanized CRC model

We previously published the therapeutic efficacy of combining oBoHV-1 with low-dose mitomycin c and ICI in a murine syngeneic model of melanoma and the importance of CD8⁺ T cells.⁸ Thus, we examined our HLA-matched humanized CRC model using this CTL-mediated combination (Comb) therapy (Figure 2(a)). Tumor regression studies showed striking tumor control with Comb compared to PBS or ICI groups (Figure 2(b–c)). While Comb also displayed activity in non-hu-mice likely due to direct cytotoxic effects (Figure S2), Comb was considerably more effective in the humanized model (Figure 2(b–c)) suggesting immune involvement.

Prior to implantation and treatment, all hu-mice had similar blood reconstitution levels (Figure 2(d)) and frequency of immune populations (Figure 2(e) and Figure S3A). There was an increase in hCD45⁺ abundance in blood following treatment with Comb at endpoint, which was not observed within tumors (Figure 2(d)). Comb treatment induced moderate weight loss, possibly due to GvHD onset (Figure S4). In blood both ICI and Comb significantly reduced the percentage of B cells, but only ICI significantly increased the percentage of

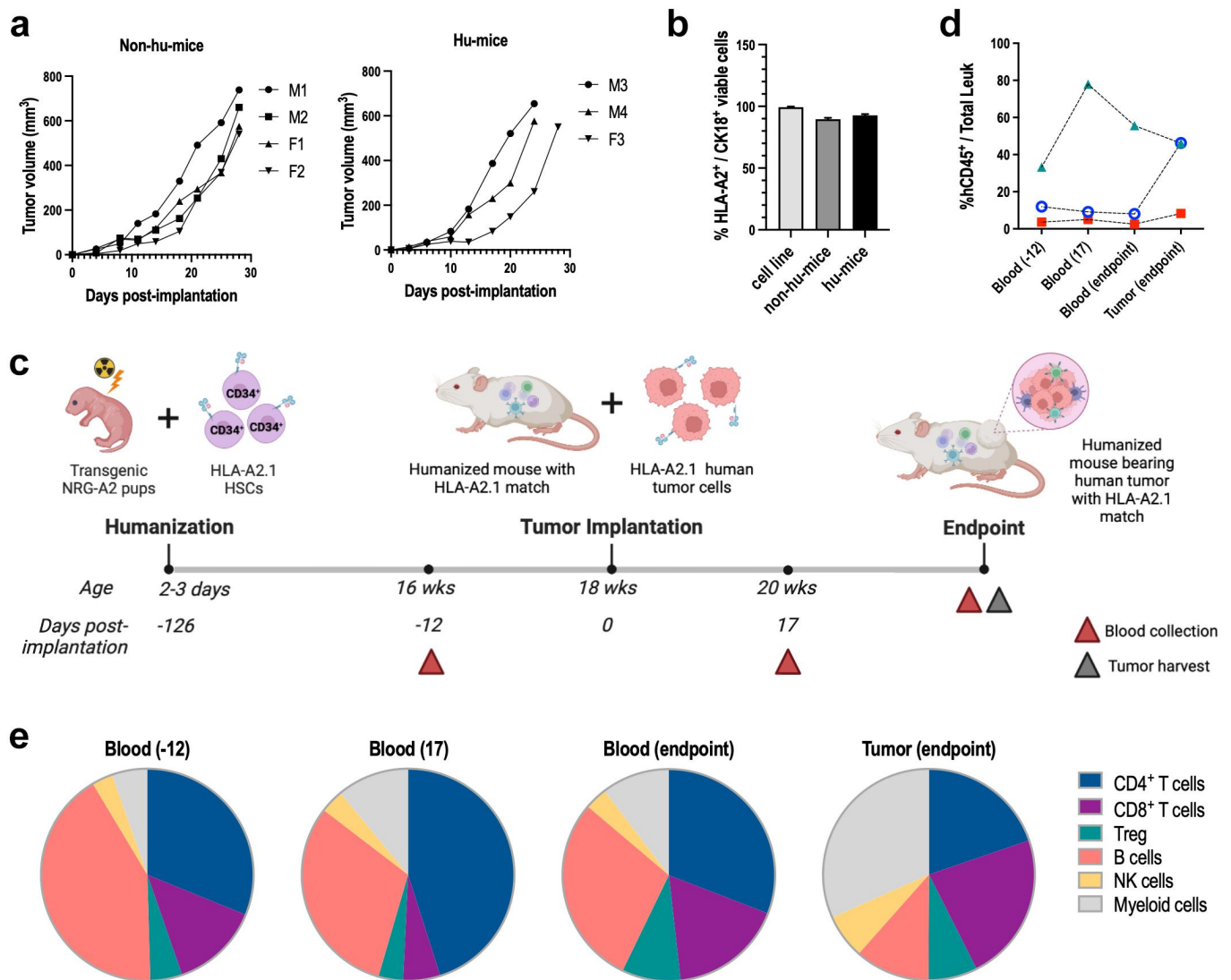


Figure 1. Humanized *KRAS*-mutated CRC model. Human colorectal cancer HCT-116 cells were implanted subcutaneously into non-humanized NRG mice (Non-hu-mice) and humanized NRG-A2 mice (Hu-mice). (a) Individual tumor volumes (Male, Female) are shown. (b) Endpoint tumors were harvested and percentage of HLA-A2⁺ cells per CK18⁺ tumor cells were analyzed by flow cytometry using HCT-116 cell line as positive control. (c) Blood of hu-mice was collected at 16 weeks (12 days pre-implantation), 20 weeks (17 days post-implantation) and at endpoint. Reconstitution levels per mouse (red square: M3; blue circle: M4; green triangle: F3) as % hCD45⁺ per total leukocytes (d) and immune cell abundance (e) were analysed in blood and tumors by flow cytometry (Figure S1).

CD8⁺ T cells (Figure 2(e) and Figure S3B). Only Comb significantly reduced tumor-infiltrating Tregs (Figure 2(e) and Figure S3C), enhancing the CTL:Treg ratio (Figure 2(f)). Moreover, Comb reduced the level of exhausted Tim3⁺ CTLs (Figure 2(g)) and highly immunosuppressive Tim3⁺ Tregs (Figure 2(h)), indicating critical activity at the tumor site.

Finally, splenic CTLs were isolated from Comb-treated hu-mice to evaluate their tumor-specific activation and confirm HLA-A2.1 restriction. CTLs were co-cultured with HCT-116 cells in the absence or presence of α HLA-A2 antibody or with HCT-HLAko cells (wt, wt + α HLA and HLAko, respectively, Figure 2(i-j)). After 4 h co-culturing, flow cytometry determined percentage of HLA-A2⁺ tumor cells (Figure 2(i)) and tumor-specific CTL activation using CD69, GrB and Ki67 (Figure 2(j)). Similar CTL:tumor cell ratios between the three experimental conditions were confirmed (Figure S5A). While α HLA-A2 effectively blocked HLA-A2.1 molecules on HCT-116 cells without CTLs (Figure S5B), only partial blocking was

observed with CTLs (Figure 2(i)). Knocking out HLA-A2.1 eliminated HLA-A2.1 expression on HCT-116 (Figure 2(i) and Figure S5b). A significant reduction of CTL CD69, GrB and Ki67 expression was observed following co-culture with HCT-HLAko cells compared to HCT-116 wt (Figure 2(j)), demonstrating CTLs isolated from Comb-treated hu-mice were tumor-specific and HLA-restricted. CTLs incubated with partial HLA-A2.1-blocked HCT-116 cells (wt + α HLA) presented an intermediate activation (Figure 2(j)).

Combination (immuno)therapy in humanized PDAC model

For the humanized model of PDAC, CFPAC-1 cells expressing *KRAS*^{G12V} and HLA-A2.1¹² were used. Implantation and HLA-A2.1 expression stability were confirmed in non-hu-mice (Figure S6). Then, humanized and non-humanized mice bearing CFPAC-1 tumors were treated with PBS, ICI or Comb. Comb significantly controls tumor growth in both hu-mice

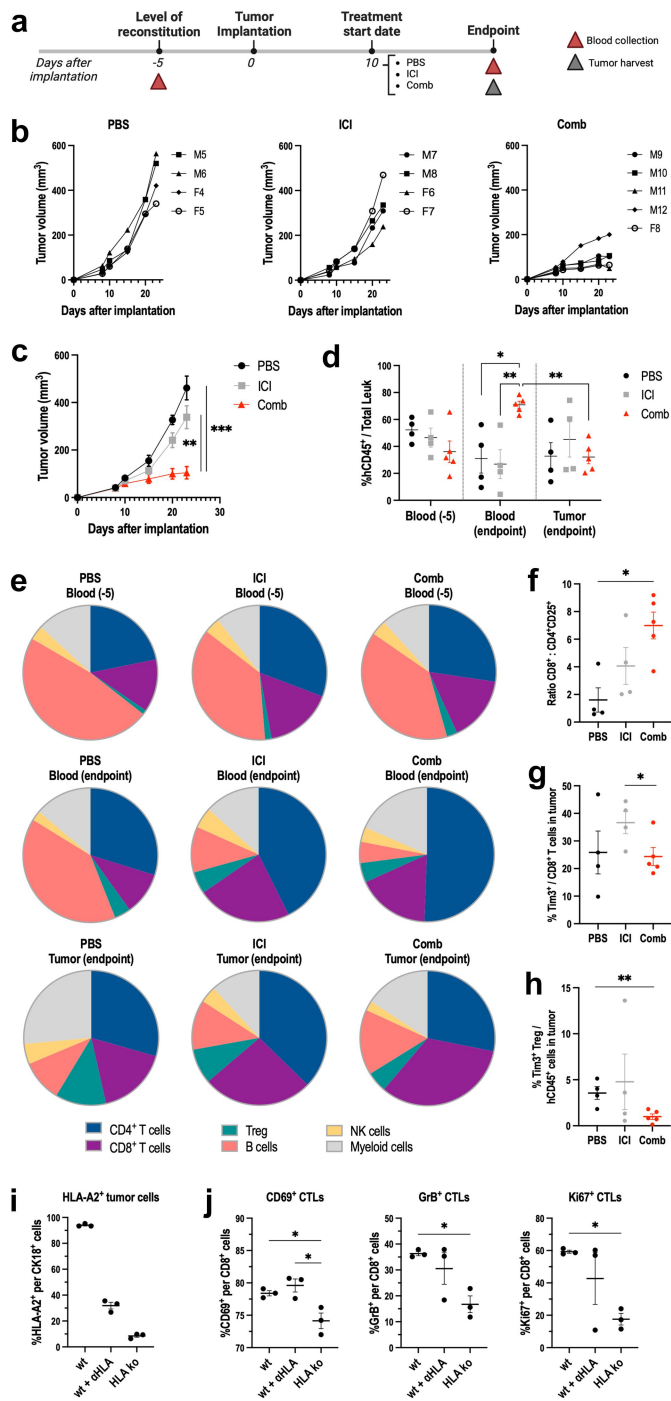


Figure 2. Combination (immuno)therapy in human *KRAS*-mutated CRC model. (a) Five days after confirming reconstitution (–5), HCT-116 cells were implanted in hu-mice (day 0). 10 days later, tumors were treated with PBS, ICI (human α -CTLA-4 and α -PD-1 from day 11 every 3 days until 10 doses total) or Comb (100 μ g MMC at day 10; 2×10^7 pfu oBoHV-1 i.t. At days 11, 14 and 17; and human ICI as described above).^{9,10} Blood and tumors were collected as indicated. Individual tumor volumes (Male, Female) (b) and group averages (c) are shown. Reconstitution levels (d) and immune cell abundance (e–h) were analysed by flow cytometry (Figure S3). Endpoint splenic CTLs from Comb-treated hu-mice were co-cultured with HCT-116 cells in the absence (wt) or presence (wt + α HLA) of α HLA-A2 antibody or with HCT-HLAko cells. HLA-A2 expression on tumor cells (i) and CD69, GrB and Ki67 expression in CTLs (j) were assessed by flow cytometry. * $p < 0.05$, ** $p < 0.01$ and *** $p < 0.001$.

(Figure 3(a–b)) and non-hu-mice (Figure S7) with better tumor control in hu-mice (Figure 3(a–b)). No significant tumor control was seen with ICI (Figure 3(a–b) and Figure

S7). As human PDAC tumors are highly complex with massive necrotic areas and a desmoplastic stroma,¹⁵ we investigated whether our model mimics this phenotype by H&E staining (Figure 3(c)) and MIBI-TOF (Figure 3(d–f)). Tumor necrosis is visualized in whole tumor sections by H&E staining as light pink areas (Figure 3(c) – black square). Evaluation of whole tumor slices revealed differences in tumor size and relative abundance and localization of necrotic tissue between treated tumors (Figure 3(c)). Elongated fibroblasts (black arrows) mixed with tumor epithelium (white arrows) characteristic of the desmoplastic stroma of PDAC were also identified in all groups (Figure 3(c)).

To further study the TME, we used MIBI-TOF which probes the microenvironment of pathological tissues at the single-cell level.¹¹ A panel consisting of 34 markers for common immune lineages and stroma (Table S6) identified 7 different cell types (Figure 3(e)). Spectral images (Figure 3(d)) and UMAP clustering (Figure 3(e)) show a reduction in panCK⁺ tumor cells (green) and CD56⁺ α -smooth muscle actin (α -SMA⁺) stroma (possibly pancreatic stellate cells (PSCs) or cancer associated fibroblasts (CAFs), orange) in Comb-treated tumors. Few immune cells were found in Comb-treated tumors, possibly due to the late harvesting timepoint, while general stroma (turquoise) remained prevalent (Figure 3(e)). Ki67 expression confirmed Comb-mediated reduced proliferation of tumor and CD56⁺ α -SMA⁺ stroma cells but not general stromal tissue (Figure 3(f)). MIBI spatial analysis further determined four distinctive regions (CN1–4 – Figure 3(g)). Most cells in Comb-treated tumors are surrounded by stroma cells (CN4 – pink region) while PBS- and ICI-treated tumors present more diversity as shown in the UMAPs color-coded by regions in Figure 3(g).

Discussion

The need for improved *in vivo* cancer models that better recapitulate the crosstalk between human tumor cells and the TME is urgent for pre-clinical immuno-oncology research.³ Hu-mouse models with human tumors and human immune components are promising. However, one major limitation of current HSC-derived humanized cancer models is the lack of a human thymus for HLA-based education of human T cell populations.^{4,16} While the BLT-hu-mouse model transplants human fetal thymus and liver into HSC-derived hu-mice, this model is highly complex and human fetal tissues are scarce. Another approach is engrafting HLA-matched human immune components into transgenic mice expressing the same HLA molecules.⁶ While many studies have shown enhanced development and survival of human CD8⁺ and CD4⁺ T cells in hu-mice with HLA-match,^{4,6,7} only one study used HLA-matched hu-mice for cancer investigation.¹⁷ Ehx *et al.* compared NSG vs transgenic NSG-HLA-A2/HHd mice humanized with PBMCs (HLA-A2.1⁺) that were engrafted with human THP-1 leukemia cells (HLA-A2.1⁺).¹⁷ Expression of HLA-A2.1 by hu-mice reduced HLA-A2.1⁺ leukemic cells but increased severe GvHD.¹⁷ We suspect both effects were caused by the high level of already mature T cells that would be avoided by using CD34⁺ HSCs instead of PBMCs

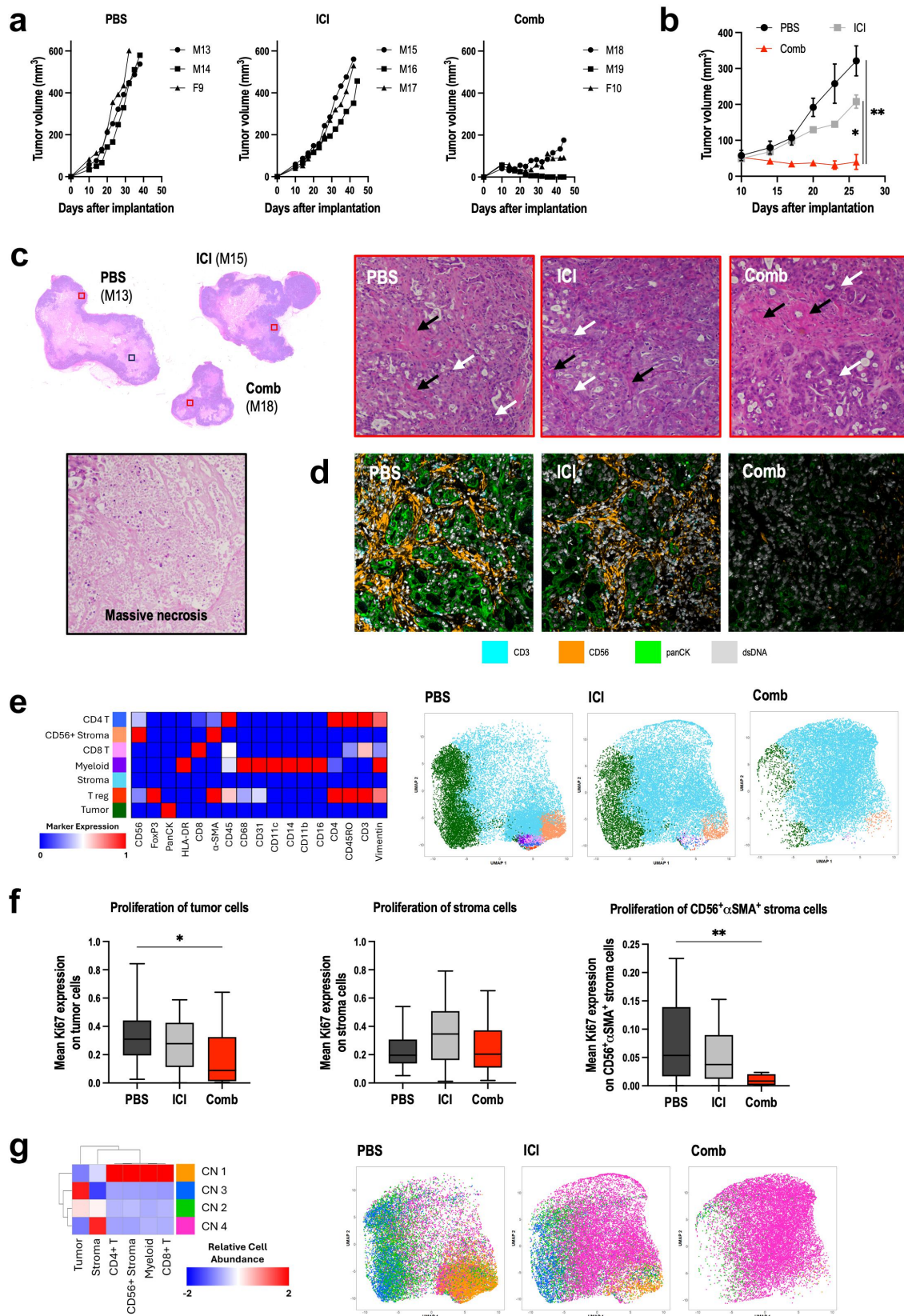


Figure 3. Combination (immuno)therapy in humanized *KRAS*-mutated PDAC model. Six days after confirming reconstitution, CFPAC-1 cells were implanted in hu-mice, and 10 days later tumors were treated with PBS, ICI (human α -CTLA-4 and α -PD-1 antibodies) or Comb (MMC + oBoHV-1 + ICI). Tumor volumes were measured every 3 days, and tumors were harvested and fixed at endpoint. Individual tumor volumes (Male, Female) (a) and group averages (b) are shown. (c) H&E histology: upper left panel has representative images of whole tumor sections for each group, with a 20 \times image of the necrotic area in the PBS-treated tumor shown below. Upper right panel shows 20 \times images of the desmoplastic stroma in PBS-, ICI- or Comb-treated tumors (black arrows – fibroblasts; white arrows – tumor epithelia). (d-g) MIBI-TOF images and analysis. (d) Representative spectral images for each group. (e) Heatmap displaying normalized individual marker expression to determine cell phenotypes presented in tumor samples, and UMAPs color-coded by cell phenotype. (f) Ki67 expression in tumor, stroma and CD56 $^{+}$ α SMA $^{+}$ stroma cells shown as a measure of proliferation. (g) Heatmap displaying relative cell abundance of each cell type in each region CN1–4, and UMAPs color-coded by regions. * $p < 0.05$ and ** $p < 0.01$.

for humanization. Here, we used CD34⁺ HSCs (HLA-A2.1⁺) to humanize transgenic NRG-A2 mice that were then engrafted with two *KRAS*-mutated cancers expressing HLA-A2.1. We chose a class I HLA due to its role in antigen-specific activation of CTLs, key immunotherapy mediators, including our combination (immuno)therapy. Although HLA-A2.1 is the most frequently detected HLA-A2 allele in all ethnic groups, different class I HLAs should be evaluated to better represent all races and ethnicities.¹⁸ Here, we present the successful engraftment and growth of *KRAS*-mutated CRC and PDAC tumors in hu-mice with HLA-class-I-match without losing HLA-A2.1 surface expression. We demonstrate that having HLA-A2.1 expressed in mouse tissue resulted in HLA-A2.1-restricted CTLs as previously reported.⁷ While an even better model would match both class I and II HLAs,⁶ identifying tumor cells or patient-derived xenografts and HSCs with the same HLA class I and II subtypes would be challenging.

After establishing two novel humanized cancer models, we evaluated their potential in immuno-oncology research by studying changes in the tumor and TME after treating with PBS, ICI (αPD-1 and αCTLA-4), or a published CTL-mediated combination (immuno)therapy⁸ (Comb) that includes ICI. The CRC model presented the characteristic immune “cold” signature of human CRC with low anti-tumor T cell infiltration that makes it resistant to ICI.¹⁹ Comb treatment elevated CTL:Treg ratios while reducing Tim3⁺ Tregs, correlating with therapeutic efficacy similar to clinical evidence.^{20,21} As opposed to other cancer types, in human CRC increased infiltrating Tregs correlates with both improved or worsened prognosis and overall survival, but highly immunosuppressive phenotypes, such as Tim3⁺ Treg, are found to be crucial in tumor immune escape.²¹ We further demonstrated that Comb activates tumor-specific HLA-restricted CTLs.

In the humanized PDAC model, a complex architecture of necrosis and desmoplastic stroma similar to human PDAC¹⁵ was seen in harvested tumors. Therapeutic efficacy of Comb correlates with reduction of extended histological necrotic areas as observed clinically.²² Moreover, Comb reduced the amount and proliferation of tumor cells and stroma cells expressing CD56, or neural cell adhesion molecule, a marker of perineural invasion of all periaampullary cancers.²³ Patients with high expression of CD56 in periaampullary tumors have reduced survival.²³ Of interest, the CD56⁺ stroma population also expresses α-SMA, a well-known activation marker of PSCs,²⁴ quiescent fibroblast-like cells that can differentiate to CAFs. High expression of α-SMA is a well-established marker of myofibroblastic CAFs, a population typically associated with tumor-restraining properties, but also with tumor-promoting capabilities in PDAC patients.²⁵

In conclusion, we successfully established two novel *KRAS*-mutated cancer models in HSC-derived hu-mice with HLA-class-I match between mouse tissue (including thymus), human immune system and human tumor that makes the model more clinically relevant compared to currently used humanized cancer models where CD8⁺ T cells are educated in the presence of mouse MHC class I molecules. Both humanized models were able to recreate the complexity and plasticity in the TME seen in patients' biopsies after treatment success or failure. Accordingly, these

models may represent an improved bridge between pre-clinical and clinical studies on human immune responses, accelerating the development of new CTL-mediated immunotherapies.

Acknowledgments

We thank Dr Ali Ashkar (McMaster University, Canada) for gifting the NRG-A2 mice and Mary Jo Smith (McMaster Immunology Research Centre Histology Facility, Canada) for histology services. Timelines were created with BioRender.com.

Disclosure statement

No potential conflict of interest was reported by the author(s).

Funding

This work was supported by the Canadian Institutes for Health Research, grant number [PJT-178174] and the Ontario Institute for Cancer Research, grant [P.CTP.1241].

ORCID

Karen L. Mossman  <http://orcid.org/0000-0002-1725-5873>

Author contributions

Conceptualization, M.E.D., A.G. and K.M.; methodology, M.E.D., J.M., J. B. and A.G.; validation, M.E.D., O.C., M.L., J.M.; formal analysis, M.E.D., M.L., and J.M.; investigation, M.E.D., O.C., M.L., J.M., J.A.H., C.S. and S. C.; resources, J.B., A.G. and K.M.; writing – original draft preparation, M. E.D.; writing – review and editing, all authors; visualization, M.E.D. and J. M.; supervision, M.E.D., J.B., A.G. and K.M.; project administration, M.E. D., A.G. and K.M.; funding acquisition, M.E.D., A.G. and K.M. All authors have read and agreed to the published version of the manuscript.

Data availability statement

The authors confirm that the data supporting the findings of this study are available within the article and its supplementary materials. Raw data and derived data supporting the findings of this study that were generated at Multiplexed Ion-Beam Imaging (MIBI) facility at McMaster University are available from the corresponding author [K.M.] on request.

References

1. Alese OB, Wu C, Chapin WJ, Ulanja MB, Zheng-Lin B, Amankwah M, Eads J. Update on emerging therapies for advanced colorectal cancer. *Am Soc Clin Oncol Educ Book*. 2023;43(43): e389574. doi:10.1200/EDBK_389574.
2. Timmer FEF, Geboers B, Nieuwenhuizen S, Dijkstra M, Schouten EAC, Puijk RS, de Vries JJJ, van den Tol MP, Bruynzeel AME, Streppel MM, et al. Pancreatic cancer and immunotherapy: a clinical overview. *Cancers (Basel)*. 2021;13(16):4138. doi:10.3390/cancers13164138.
3. Hegde PS, Chen DS. Top 10 challenges in cancer immunotherapy. *Immunity*. 2020;52(1):17–35. doi:10.1016/j.immuni.2019.12.011.
4. Chuprin J, Buettner H, Seedhom MO, Greiner DL, Keck JG, Ishikawa F, Shultz LD, Brehm MA. Humanized mouse models for immuno-oncology research. *Nat Rev Clin Oncol*. 2023;20(3):192–206. doi:10.1038/s41571-022-00721-2.
5. Ashizawa T, Iizuka A, Nonomura C, Kondou R, Maeda C, Miyata H, Sugino T, Mitsuya K, Hayashi N, Nakasu Y, et al. Antitumor effect of programmed death-1 (PD-1) blockade in

- humanized the NOG-MHC double knockout mouse. *Clin Cancer Res.* **2017**;23(1):149–158. doi:10.1158/1078-0432.CCR-16-0122.
6. Lepard M, Yang JX, Afkhami S, Nazli A, Zganiacz A, Tang S, Choi MWY, Vahedi F, Deshiere A, Tremblay MJ, et al. Comparing current and next-generation humanized mouse models for advancing HIV and HIV/Mtb Co-infection studies. *Viruses.* **2022**;14(9):1927. doi:10.3390/v14091927.
 7. Shultz LD, Saito Y, Najima Y Tanaka S, Ochi T, Tomizawa M, Doi T, Sone A, Suzuki N, Fujiwara H, et al. Generation of functional human T-cell subsets with hla-restricted immune responses in HLA class I expressing NOD/SCID/IL2ry^{null} humanized mice. *Proceedings of the National Academy of Sciences*; Vol. 107. **2010**. p. 13022–13027. doi:10.1073/pnas.1000475107.
 8. Davola ME, Cormier O, Vito A, El-Sayes N, Collins S, Salem O, Revill S, Ask K, Wan Y, Mossman K. Oncolytic BHV-1 is sufficient to induce immunogenic cell death and synergizes with low-dose chemotherapy to dampen immunosuppressive T regulatory cells. *Cancers.* **2023**;15(4):1295. doi:10.3390/cancers15041295.
 9. Rios-Doria J, Stevens C, Maddage C, Lasky K, Koblish HK. Characterization of human cancer xenografts in humanized mice. *J Immunother Cancer.* **2020**;8(1):e000416. doi:10.1136/jitc-2019-000416.
 10. Küçükköse E, Heesters BA, Villaudy J, Verheem A, Cercel M, van Hal S, Boj SF, Borel Rinkes IHM, Punt CJA, Roodhart JML, et al. Modeling resistance of colorectal peritoneal metastases to immune checkpoint blockade in humanized mice. *J Immunother Cancer.* **2022**;10(12):e005345. doi:10.1136/jitc-2022-005345.
 11. Chokshi CR, Shaikh MV, Brakel B, Rossotti MA, Tieu D, Maich W, Anand A, Chafe SC, Zhai K, Suk Y, et al. Targeting axonal guidance dependencies in glioblastoma with ROBO1 CAR T cells. *Nat Med.* **2024**;30(10):2936–2946. doi:10.1038/s41591-024-03138-9.
 12. Scholtalbers J, Boegel S, Bukur T, Byl M, Goerges S, Sorn P, Loewer M, Sahin U, Castle JC. TCLP: an online cancer cell line catalogue integrating HLA type, predicted neo-epitopes, virus and gene expression. *Genome Med.* **2015**;7(1):118. doi:10.1186/s13073-015-0240-5.
 13. Wang M, Yao L-C, Cheng M, Cai D, Martinek J, Pan C-X, Shi W, Ma A-H, Vere White RW, Airhart S, et al. Humanized mice in studying efficacy and mechanisms of PD-1-targeted cancer immunotherapy. *FASEB J.* **2018**;32(3):1537–1549. doi:10.1096/fj.201700740R.
 14. Capasso A, Lang J, Pitts TM, Jordan KR, Lieu CH, Davis SL, Diamond JR, Kopetz S, Barbee J, Peterson J, et al. Characterization of immune responses to anti-PD-1 mono and combination immunotherapy in hematopoietic humanized mice implanted with tumor xenografts. *J Immunother Cancer.* **2019**;7(1). doi:10.1186/s40425-019-0518-z.
 15. Hosein AN, Brekken RA, Maitra A. Pancreatic cancer stroma: an update on therapeutic targeting strategies. *Nat Rev Gastroenterol Hepatol.* **2020**;17(8):487–505. doi:10.1038/s41575-020-0300-1.
 16. Guil-Luna S, Sedlik C, Piaggio E. Humanized mouse models to evaluate cancer immunotherapeutics. *Annu Rev Cancer Biol.* **2021**;5(1):119–136. doi:10.1146/annurev-cancerbio-050520-100526.
 17. Ehx G, Somja J, Warnatz H-J, Ritacco C, Hannon M, Delens L, Fransolet G, Delvenne P, Muller J, Beguin Y, et al. Xenogeneic graft-versus-host disease in humanized NSG and NSG-HLA-A2/HHD mice. *Front Immunol.* **2018**;9:1943. doi:10.3389/fimmu.2018.01943.
 18. Olivier T, Haslam A, Tuia J, Prasad V. Eligibility for human leukocyte antigen-based therapeutics by race and ethnicity. *JAMA Netw Open.* **2023**;6(10):e2338612. doi:10.1001/jamanetworkopen.2023.38612.
 19. Liu JL, Yang M, Bai JG, Liu Z, Wang XS. “Cold” colorectal cancer faces a bottleneck in immunotherapy. *World J Gastrointest Oncol.* **2023**;15(2):240–250. doi:10.4251/wjgo.v15.i2.240.
 20. Klapholz M, Drage MG, Srivastava A, Anderson AC. Presence of Tim3+ and PD-1+ CD8+ T cells identifies microsatellite stable colorectal carcinomas with immune exhaustion and distinct clinicopathological features. *J Pathol.* **2022**;257(2):186–197. doi:10.1002/path.5877.
 21. Aristin Revilla S, Kranenburg O, Coffey PJ. Colorectal cancer-infiltrating regulatory T cells: functional heterogeneity, metabolic adaptation, and therapeutic targeting. *Front Immunol.* **2022**;13. doi:10.3389/fimmu.2022.903564.
 22. Hiraoka N, Ino Y, Sekine S, Tsuda H, Shimada K, Kosuge T, Zavada J, Yoshida M, Yamada K, Koyama T, et al. Tumour necrosis is a postoperative prognostic marker for pancreatic cancer patients with a high interobserver reproducibility in histological evaluation. *Br J Cancer.* **2010**;103(7):1057–1065. doi:10.1038/sj.bjc.6605854.
 23. Aloysius MM, Zaitoun AM, Awad S, Ilyas M, Rowlands BJ, Lobo DN. Mucins and CD56 as markers of tumour invasion and prognosis in periampullary cancer. *Br J Surg.* **2010**;97(8):1269–1278. doi:10.1002/bjs.7107.
 24. Haerberle L, Steiger K, Schlitter AM, Safi SA, Knoefel WT, Erkan M, Esposito I. Stromal heterogeneity in pancreatic cancer and chronic pancreatitis. *Pancreatol.* **2018**;18(5):536–549. doi:10.1016/j.pan.2018.05.004.
 25. Brichkina A, Polo P, Sharma SD, Visestamkul N, Lauth M. A quick guide to CAF subtypes in pancreatic cancer. *Cancers (Basel).* **2023**;15(9):2614. doi:10.3390/cancers15092614.